bioRxiv preprint doi: https://doi.org/10.1101/240028; this version posted December 28, 2017. The copyright holder for this preprint (which was not certified by peer review) is the author/funder, who has granted bioRxiv a license to display the preprint in perpetuity. It is made available under aCC-BY-NC-ND 4.0 International license.

Development of High-Order Organization of Guanine-Based Reflectors Underlies the Dual Functionality of the Zebrafish Iris

Dvir Gur[1 2], Jan-David Nicolas[3], Vlad Brumfeld[4], Omri Bar-Elli[1], Dan Oron[1], Gil Levkowitz[2]**

Affiliations:

[1]Department of Physics of Complex Systems, Weizmann Institute of Science, Rehovot, 7610001, Israel.

[2]Department of Molecular Cell Biology, Weizmann Institute of Science, Rehovot, 7610001, Israel.

[3] Institut für Röntgenphysik, Göttingen, 37077, Germany.

[4]Department of Chemical Research Support, Weizmann Institute of Science, Rehovot, 7610001, Israel.

*Correspondence to: Dan Oron <dan.oron@weizmann.ac.il> and/or Gil Levkowitz <gil.levkowitz@weizmann.ac.il>

Abstract: Many marine organisms have evolved a reflective iris to prevent unfocused light from reaching the retina. The fish iris has a dual function, both to camouflage the eye and serving as a light barrier. Yet, the mechanism that enables this dual functionality and the benefits of using a reflective iris have remained unclear. Using synchrotron micro-focused diffraction, cryo-SEM imaging and optical analyses on zebrafish at different stages of development, we show that the complex optical response of the iris is facilitated by the development a high-order organization of multilayered guanine-based crystal reflectors and pigments. We further demonstrates how the efficient light reflector is established during development to allow the optical functionality of the eye, already at early developmental stages. These results shed light on the evolutionary drive for developing a compact reflective iris, which are widely used by many animal species.

One Sentence Summary: The dual function of the zebrafish iris as a light barrier and camouflage reflector is enabled by the high-order organization of intracellular guanine crystals and pigments.

bioRxiv preprint doi: https://doi.org/10.1101/240028; this version posted December 28, 2017. The copyright holder for this preprint (which was not certified by peer review) is the author/funder, who has granted bioRxiv a license to display the preprint in perpetuity. It is made available under aCC-BY-NC-ND 4.0 International license.

Main Text: In the eyes of numerous organisms, including mammals, reptiles, birds and fish, light is absorbed by photoreceptors in the dorsally located retina. In order to obtain a high-contrast image, only light that passes through the pupil and is focused by the lens should reach the retina. Hence, a key function of the iris is to prevent the passage of unfocused light. Irises can be classified either as absorptive, or as reflective or scattering, according to their operating principle with regard to incident light (*1, 2*). Many irises of the absorptive type, including in the human eye, contain melanin pigments that efficiently absorb a broad spectrum of visible light (*1, 3*). An alternative strategy is employed by numerous marine organisms, in which the outer surface of the iris is highly reflective (*2, 4-8*).

The reflecting iris of many fish species consists of intracellular crystals that are formed by the nucleobase guanine (*9-12*). These guanine crystals are assembled in specialized cells, named iridophores, which are located mainly in the eyes and skin (*2, 13-15*). In addition to its function as a light barrier, the iris of fish has a second role of camouflaging the eye by creating a silvery reflection similar to that of fish skin (*2, 9, 11*). Both these functions require the iris to reflect light efficiently. However, for effective camouflage the iris should reflect light in a highly directional manner (*9, 11*), whereas to block light the iris should reflect or scatter light independently of angle or wavelength (*1, 3*).

Although the dual function of the evolutionarily conserved fish iris has long been known (*2, 11*), the underlying mechanism that enables this duality has remained unclear. Here, we unravel the unique ultrastructure of iridophores in the zebrafish iris, which comprises multilayered organization of the guanine-based crystals. We directly associate the iris crystal organization to simulated and measured reflectance spectrum. We further show that the structural organization of the developing zebrafish iris is ideally designed to reflect light efficiently at a very early stage of development, which correlates well with the reported high visual acuity of the larva. Mapping of crystal orientations across the entire iris revealed the high-order crystal organization, which enables the dual function of the iris.

bioRxiv preprint doi: https://doi.org/10.1101/240028; this version posted December 28, 2017. The copyright holder for this preprint (which was not certified by peer review) is the author/funder, who has granted bioRxiv a license to display the preprint in perpetuity. It is made available under aCC-BY-NC-ND 4.0 International license.

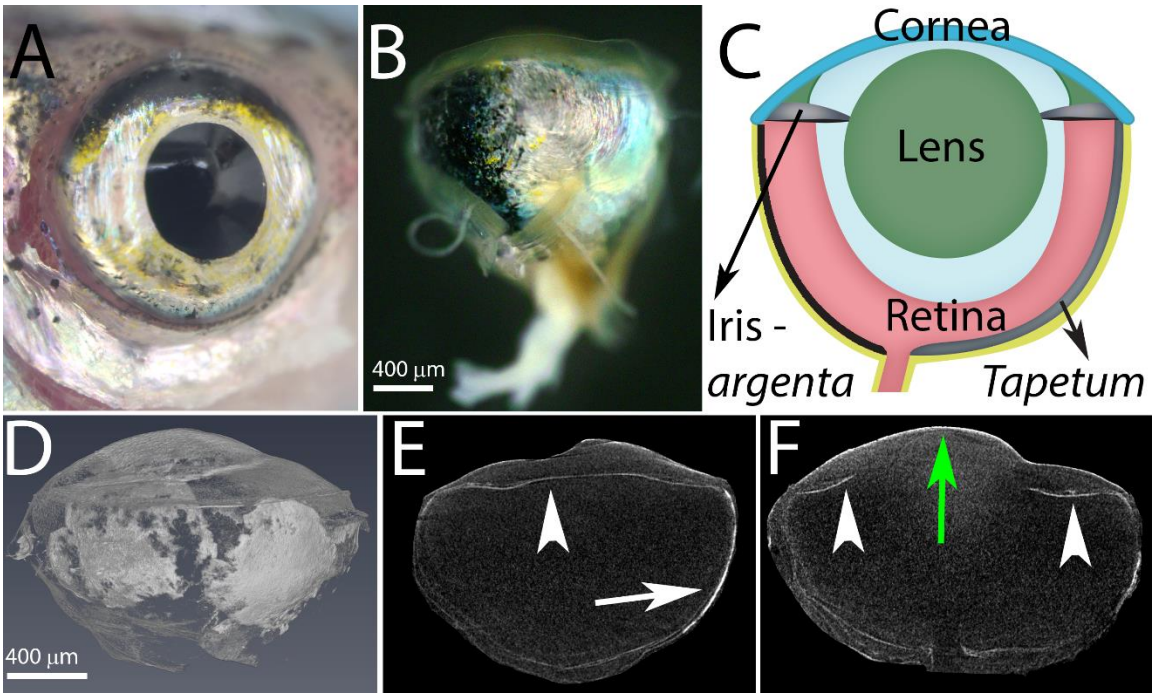

Fig. 1. The anatomy of the zebrafish eye. A) A top view of the zebrafish eye showing the silvery iris. B) A side view of the fish eyeball showing the *tapetum lucidum*, a silvery layer, located at the bottom part of the eyeball (right) and a pigmented layer visible at the upper part of the eyeball (left). C) A schematic representation of the eye showing the cornea (blue), lens (green), and retina (light red), as well as the guanine-based reflecting layers, the iris *argenta* and the *tapetum lucidum* (silver) and the pigmented layer (black). D-F) Micro-CT images of the zebrafish eye: a volume rendering of the whole eye (D), a sagittal view of the lower part of the eye (E), and a sagittal view of the center of the eye (F). Arrowheads indicate the iris *argentum*, white arrow indicates the *tapetum lucidum* and green arrow indicates the cornea. Scale bars: 400 µm.

To elucidate iris anatomy and the subcellular organization of the guanine-based reflectors, we used the zebrafish eye as a model system. In it, the lens is surrounded by a silvery iris, termed *argenta*, which is exposed to direct external light (Fig. 1, A to C). We first imaged the entire zebrafish eye using micro-CT (Fig. 1, D to F), in which the guanine-based crystal layers of the iris are clearly visible due to their high density. Serial scans showed that the zebrafish iris extends to the dorsal part of the eyeball, where it forms a reflecting mirror behind the retina, termed the *tapetum lucidum* (Fig. 1, B, C and E). The upper, outermost layer of the eye was devoid of the reflecting guanine-based layer and, instead, was covered by melanin pigments (Fig. 1B). In tomographic images of sagittal slices through the dorsal (upper) or ventral (lower) part of the eye, the iris surface appeared as a continuous layer across the entire section (Fig. 1E), whereas in a

bioRxiv preprint doi: https://doi.org/10.1101/240028; this version posted December 28, 2017. The copyright holder for this preprint (which was not certified by peer review) is the author/funder, who has granted bioRxiv a license to display the preprint in perpetuity. It is made available under aCC-BY-NC-ND 4.0 International license.

sagittal slice through the center of the eye, the two sides of the iris were separated by the lens (Fig. 1F).

To visualize the organization of the guanine-based reflectors in the adult zebrafish iris under near-physiological conditions we used cryo-SEM, which allows preservation of intact guanine crystals in their native cellular context (Fig. 2 A and B). Imaging of coronal sections through the eye revealed that the iris is composed of three different layers: an upper layer of ordered iridophores, a middle layer of disordered iridophores, and a thin layer (~5 µm) of pigment-forming melanophores, which lies beneath the two iridophore layers (Fig. 2, A and E). The cryo-SEM analysis also showed that the outermost, ordered iridophore layer was composed of monodisperse elongated hexagonal guanine crystals, which were stacked on top of each other (Fig. 2, A and C). These crystals displayed an average thickness of 25±7 nm (n=150) and an average cytoplasm spacing of 142±25 nm (n=140). In the adjacent disordered layer, the spacing between crystals was highly variable and their arrangement appeared random, with no preferred orientation (Fig. 2, A and D). Notably, the disordered iridophore layer was present only in the iris *argenta* and was missing from the *tapetum lucidum*.

We next imaged a horizontal section of the eye (Fig. 2B), where the ordered layer was seen as an array of tightly packed crystals perfectly tiling the surface of the iris. The tiling of the crystals was extremely compact, to the extent that it was difficult to separate between iridophores. These results show that in the iris of zebrafish eye, the *argenta* and *tapetum lucidum* form a continuous layer. Yet, whereas the *tapetum* is composed only from one ordered layer of iridophores, the *argenta* has a second, disordered guanine-based layer underlaid by a thin melanosome-based pigment layer.

bioRxiv preprint doi: https://doi.org/10.1101/240028; this version posted December 28, 2017. The copyright holder for this preprint (which was not certified by peer review) is the author/funder, who has granted bioRxiv a license to display the preprint in perpetuity. It is made available under aCC-BY-NC-ND 4.0 International license.

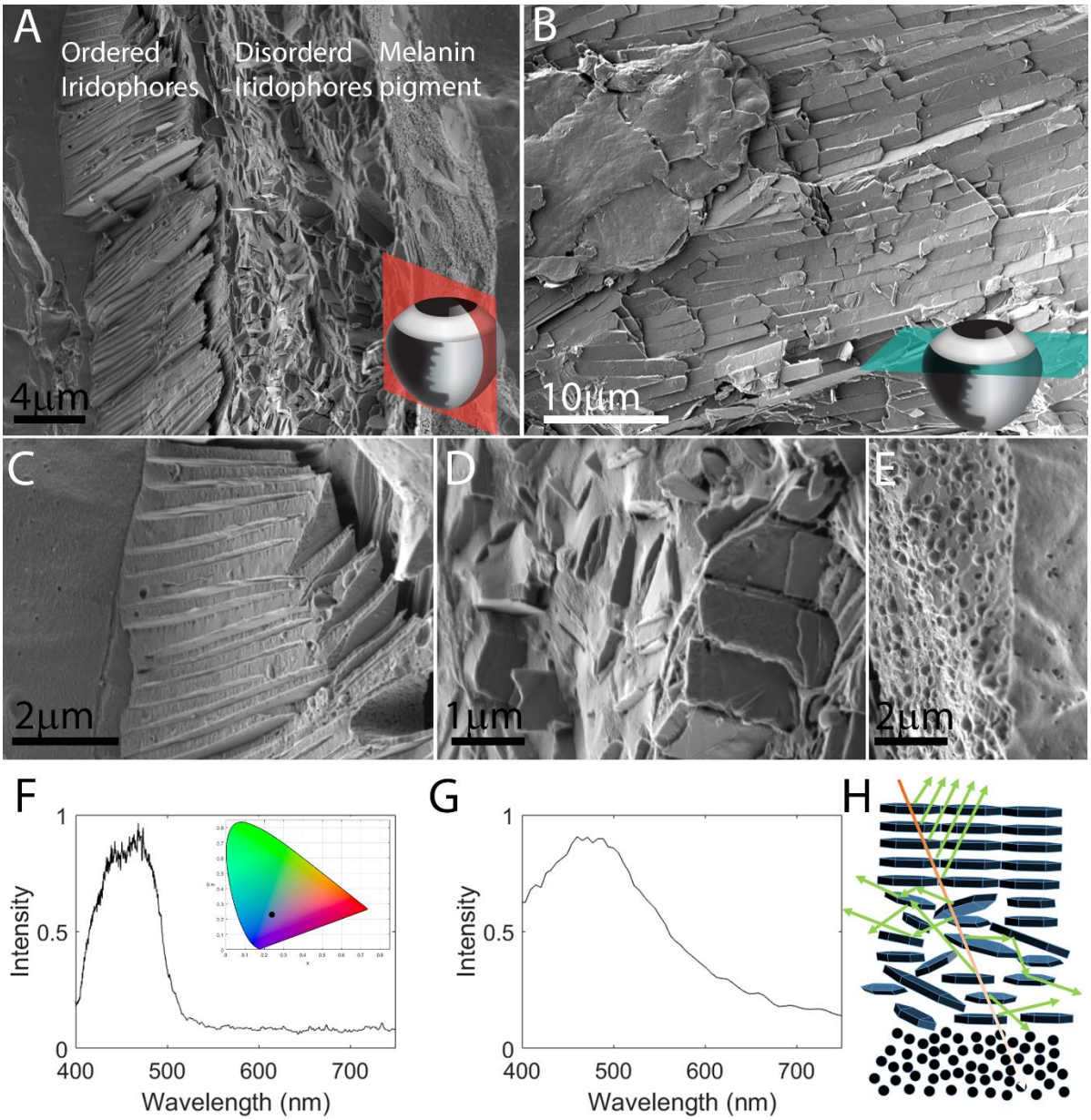

Fig. 2. The ultrastructure and optical properties of the iris. A) A coronal section through the iris showing three distinct layers: (i) ordered iridophores, (ii) disordered iridophores, and (iii) a pigmented layer. The section was taken from the periphery of the eye where the iris is curved and, thus, the crystals in the ordered layer are tilted. B) A top view of the iris obtained by a transverse section through the eye shows the elongated guanine crystals packed one next to the other, perfectly tiling the surface of the iris. The anatomical location of sections are illustrated in the bottom-right corners in A,B. C-E) Show higher magnifications of the different iris layers: ordered iridophores (C), disordered iridophores (D), and pigmented layer (E). A-E) Show Cryo-SEM micrographs of high-pressure frozen, freeze-fractured iris F) Graph showing measured reflectance from the iris, revealing a broad peak centered around 450 nm. Inset shows the color of reflected

bioRxiv preprint doi: https://doi.org/10.1101/240028; this version posted December 28, 2017. The copyright holder for this preprint (which was not certified by peer review) is the author/funder, who has granted bioRxiv a license to display the preprint in perpetuity. It is made available under aCC-BY-NC-ND 4.0 International license.

light (black dot) plotted on a 1931 CIE chromaticity space diagram. G) Simulated reflectance of the ordered layer calculated based on the data in high-resolution cryo-SEM micrographs H) A sketch illustrating the different paths of light traveling through the multi-layered iris. Scale bars: 4 µm (A), 10 µm (B), 2 µm (C,E), 1 µm (D).

Next, we hypothesized that the three-layer composition of the iris underlies a complex optical response, which combines wavelength-dependent light reflection, scattering and absorption. Because impinging light will first hit the reflectors of the outermost layer of the iris, we assumed that the majority of light would be reflected from the ordered layer. To simulate the reflectance of the ordered layer, we analyzed our cryo-SEM data, namely the spacing between crystals, using the Monte Carlo transfer matrix method (see Materials and Methods). The analysis showed that the ordered layer mostly reflects blue-green light, which peaked at 450 nm (Fig. 2G). To correlate our simulated results with actual optical measurements, we used a custom-built light microscope equipped with a spectrophotometer. Indeed, spectral measurements showed that approximately 80-90% of the blue-green light was reflected from the iris (Fig. 2F). The agreement between simulated calculations and optical measurements suggests that the majority of the blue-green light is indeed reflected from the ordered iridophore layer of the zebrafish iris.

Based on the combined results of ultrastructure imaging, light reflectance simulations and real-time optical measurements, we propose a model for light traveling through the iris (Fig. 2H). The ordered iridescent layer reflects approximately 80-90% of the impinging blue-green light. The residual light that passeses through the first layer is scattered by the disordered layer. Finally, the thin pigmented layer likely absorbs any light passing the two guanine-based layers, including light that is forward-scattered from the disordered layer. In addition, the scattering of light by the disordered layer, as it likely introduce an angular spread to the incoming light, increases the probability for light to be absorbed by the melanin pigment.

Zebrafish reproduce by external fertilization, which means that the offspring must be self-sufficient very early in life. High visual acuity is pertinent to the survival of free-swimming zebrafish, which rely on visual stimuli for prey capture (*16-18*). Previous studies showed that iridophores in zebrafish iris could be detected as soon as 3dpf (*7*). We therefore predicted that the zebrafish iris would be highly functional at early developmental stages. To test this hypothesis, we analyzed the optical properties, iridophore ultrastructure and crystal organization of the zebrafish

bioRxiv preprint doi: https://doi.org/10.1101/240028; this version posted December 28, 2017. The copyright holder for this preprint (which was not certified by peer review) is the author/funder, who has granted bioRxiv a license to display the preprint in perpetuity. It is made available under aCC-BY-NC-ND 4.0 International license.

iris at different stages of development. Light microscopy revealed that iridophores were indeed clearly visible in the iris already at 3 days post fertilization (dpf), where they intially occupy the inner circumferential layer, lining the inner radius of the iris around the lens (Fig. S1). At 7 dpf, iridophores covered only about half of the iris surface (Fig. 3A). At 14 dpf, the iridophores occupied a larger area of the iris; however, large dark patches showing the underling pigmented layer, were still visible. By 21 and 28 dpf, the iridophores covered nearly the entire surface of the iris (Fig. 3, E and G).

To elucidate the development of the iris ultrastructure, we performed cryo-SEM imaging at corresponding development stages. We found that at 7 dpf, the guanine crystals in the clearly visible iridophores were arranged in relatively ordered parallel stacks, similar to the adult iris (Fig. 3B). However, at this stage, only one layer of iridophores was visible. Moreover, individual crystals were smaller than those observed in adults and, in certain cases, the membranes engulfing the crystal seemed less tight than in adults (Fig. 3B). At 14 dpf, still only one layer of iridophores was present, but the crystal stacks were more ordered compared to 7 dpf (Fig. 3D). By 21 dpf, iris thickness increased considerably and the second layer of iridophores was sometimes visible, usually in the areas closest to the lens (Fig. S2). At this age, guanine crystals and iridophore ultrastructure resembled those of adult fish, suggesting that the iris is already fully functional as a reflecting light barrier.

To determine the functionality of the iris during development, we measured the reflectance spectrum at corresponding stages (Fig. 3H). Despite the incomplete crystal layers and iridophore coverage at larval stages, a wide reflectance peak centered on 450 nm wavelength was measured from a very early stage (7 dpf) until adulthood (Fig. 3H). The reflectance intensity increased with age, averaging at ~40% for 7 dpf larva and reaching ~80% by 28 dpf, very close to the levels observed in adults. Taken together, these results indicate that the larval iris functions as an efficient light-barrier already at 7 dpf, and that this initial functionality is preserved and optimized throughout eye development. These findings are consistent with the reported high visual acuity of very early stage zebrafish larvae (*16-18*).

bioRxiv preprint doi: https://doi.org/10.1101/240028; this version posted December 28, 2017. The copyright holder for this preprint (which was not certified by peer review) is the author/funder, who has granted bioRxiv a license to display the preprint in perpetuity. It is made available under aCC-BY-NC-ND 4.0 International license.

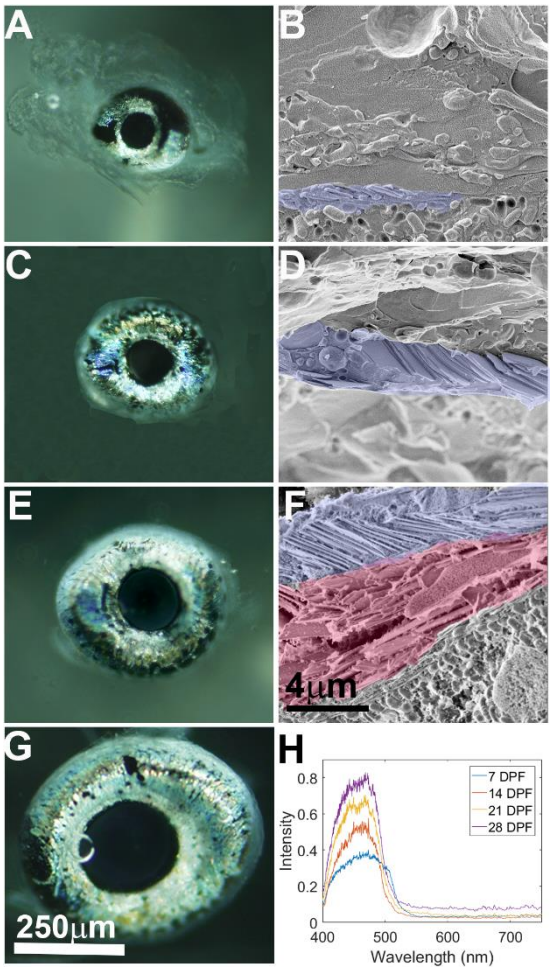

Fig. 3. Iris development. Iris morphology, ultrastructural and optical properties were examined during development at 7 (A,B), 14 (C,D), 21 (E,F) and 28 (G) dpf. A,C,E,G) Light microscope images of the larva iris at different stages. B,D,F) Cryo-SEM micrographs of high-pressure frozen, freeze-fractured larva iris show the ultrastructure of the developing iris. Whereas at 7 and 14 dpf only the ordered layer is seen, by 21 dpf a second, disordered layer starts to appear. Ordered iridophores (purple) and disordered iridophores (light red) are shown in pseudo-colors H) Graph showing measured reflectance of irises from 7, 14, 21 and 28 dpf larvae, revealing a peak reflectance centered around 450 nm. Scale bars: 250 µm (A,C,E,G), 4 µm (B,D,F).

Having found that light is reflected mostly from the outermost ordered iridophore layer, we hypothesized the existence of an intrinsic, high-order organization of crystal stacks within this layer. To examine this, we sought to map the orientation of the guanine crystals stacks across the entire iris. Because the adult zebrafish iris is composed of millions of crystals extending across several square millimeters, mapping crystal orientations accurately using high-resolution imaging techniques such as cryo-SEM was not feasible, whereas modalities for imaging relatively large

bioRxiv preprint doi: https://doi.org/10.1101/240028; this version posted December 28, 2017. The copyright holder for this preprint (which was not certified by peer review) is the author/funder, who has granted bioRxiv a license to display the preprint in perpetuity. It is made available under aCC-BY-NC-ND 4.0 International license.

areas, such as micro-CT, would not provide sufficient resolution to determine the orientation of individual stacks. Therefore, we opted to use scanning x-ray diffraction combined with a micro-focused synchrotron beam. Thus, the x-ray beam continuously scanned across the sample and the diffraction patterns were collected with a single-photon counting flat panel detector at regular time intervals. The scanning speed was set such that a diffraction pattern was collected every 4 µm. Thus, a single scan could contain over 400,000 diffraction patterns, covering the entire surface area of the iris at an overall scan time of about 1 hour per sample. To analyze the data in a standardized, robust and model-independent fashion, we used a custom Matlab-based principal component analysis (PCA) based on Bernhardt et al. (*19*) as part of a Nano-diffraction toolbox Nicolas et al (*20*) (Materials and Methods, supporting information). Using this PCA algorithm, we extracted the anisotropy and orientation of light scattering and, subsequently, inferred the orientation of the crystals.

Based on our TEM studies (Fig. S3), the crystals in the fish iris are anhydrous β-guanine (100) crystal plates, (Fig. 4C). Thus, the (100) plane is in diffraction for crystals that are oriented almost edge-on to the beam (see Fig. 1A color bar for crystal orientation). Mapping the anisotropy and orientation of the (100) diffraction plane revealed two regions of crystal stacks, an inner layer that surrounded the lens and an outer layer surrounding the outer radius of the eye (Fig. 4A). The crystals in the two layers were positioned tangent to the iris circumference, lining the top section of the eye. Remarkably, the orientation of the crystal stacks at the inner and outer radii followed the curvature of the iris (Fig. 4A). In the outer layer, the crystals extended up to the point where the eye is protruding out from the fish head, suggesting that they prevent light that impinges upon the eye from the side from distorting the fish vision (Fig. 4F and Fig. S4). Accordingly, the crystals at the inner layer, which surrounds the lens, would reflect light that is impinged upon the lens sideways, and thus limit the angular acceptance of the eye, leading to a reduction in spherical aberrations. This inner circumference layer may also provide a tighter seal for light at the interface between the lens and the iris (Fig. 4F).

The perpendicular (002) plane should only be in diffraction for crystals that are positioned almost perpendicular to the beam (Fig. 4C). Mapping the (002) diffraction plane across the iris showed that the orientation of most of the crystals was parallel to the iris surface (Fig. 4D), suggesting that they would efficiently reflect light impinging on the surface (Fig. 4F). Due to the

bioRxiv preprint doi: https://doi.org/10.1101/240028; this version posted December 28, 2017. The copyright holder for this preprint (which was not certified by peer review) is the author/funder, who has granted bioRxiv a license to display the preprint in perpetuity. It is made available under aCC-BY-NC-ND 4.0 International license.

curvature of the iris close to its periphery, the crystal were tilted and were thus out of diffraction. Nonetheless, these regions are still tiled by crystals, as observed by mapping the diffraction of all the different crystal planes, regardless of their orientation (Fig. S4B).

Remarkably, the crystals that tile the surface of the iris were aligned throughout the entire iris, covering several square millimeters in adult fish. This co-orientation of crystals across tens of thousands of cells suggests that the concerted organization of crystals is highly regulated. Presumably, cell communication between iridophores facilitates orienting the crystals across the iris in a synchronized manner. Such coordinated cell communication mechanism was previously reported for other types of pigment cells during zebrafish color pattern formation (*21*-*24*). Light reflection from a flat layer of co-orientated crystals could be analogous to the specular reflection from a flat mirror, which is characterized by a high degree of directionality. Indeed, Fourier transform reflection analysis indicated that reflection from the iris is highly directional (Fig. S6).

In zebrafish, the eyes are located on both sides of the head such that the iris surfaces are at an oblique angle to impinging sunlight. Thus, sunlight should be reflected from the iris at an obtuse angle, preserving the down welling direction of the light. This may be beneficial for camouflage in shallow waters, where upwelling iridescence is relatively minute (*25*). Thus, light reflected or scattered in any direction other than downwelling would be highly conspicuous, revealing the location of the fish to potential predators. Furthermore, the co-orientation of the crystals may allow perfect surface tiling and, thus, minimize surface defects. Such defects may lead to transmission of light through the iris and onto the retina, reducing the contrast of the obtained image.

bioRxiv preprint doi: https://doi.org/10.1101/240028; this version posted December 28, 2017. The copyright holder for this preprint (which was not certified by peer review) is the author/funder, who has granted bioRxiv a license to display the preprint in perpetuity. It is made available under aCC-BY-NC-ND 4.0 International license.

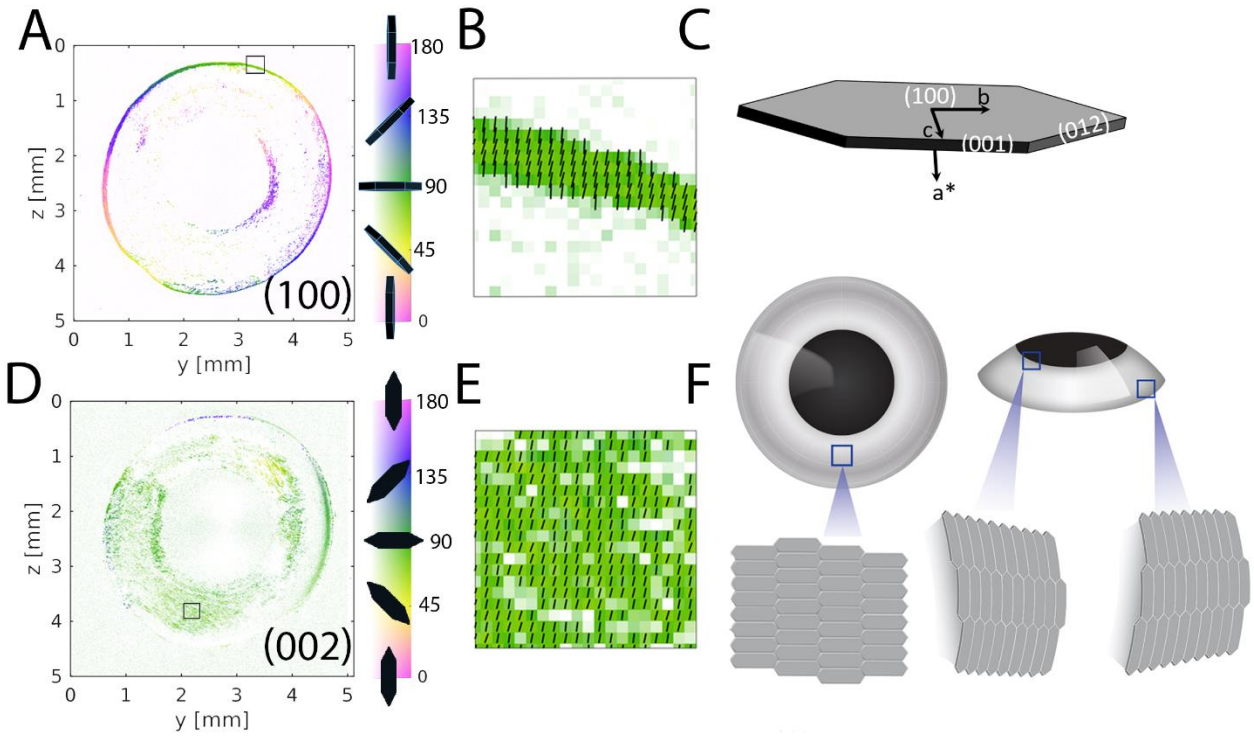

Fig. 4. Synchrotron-based diffraction imaging. The orientation of the different crystal planes was mapped across the entire iris using scanning x-ray diffraction combined with a micro-focused synchrotron beam. A,D) Maps showing the orientations of the (100) and (002) guanine crystal diffraction planes, respectively. The color gradient (right bar) from white to saturated color corresponds to the respective low and high anisotropy levels. B,E) Magnifications of the squared regions marked in (A) and (D), respectively. C) Schematic illustration of fish guanine crystal, showing the relations between crystal morphology and the crystallographic axes and faces. F) Schematic illustration showing the orientations of the guanine plate-like crystals at different regions of the eye.

Having both an ordered and a disordered layer enables the dual functionality of the iris, an efficient light barrier that also provides camouflage to the normally black uveal tract. The first ordered layer is an efficient directional light reflector and, at most angles, incident light will be reflected efficiently. However, at very obtuse angles, at which light is almost parallel to the reflectors (for example, sunlight scattered by an object in the water), or when light is at the red edge of the visible spectrum, the efficiency of the reflectors is reduced dramatically. Having a second layer of varying crystal orientations could provide a solution to this problem. A second functional benefit for having two iris layers relates to the spectral environment of the eye. In the marine environment, the longer wavelengths are rapidly absorbed in the water, leaving mostly blue-green light (*25*, *26*). Furthermore, the opsins in the zebrafish retina are much more sensitive

bioRxiv preprint doi: https://doi.org/10.1101/240028; this version posted December 28, 2017. The copyright holder for this preprint (which was not certified by peer review) is the author/funder, who has granted bioRxiv a license to display the preprint in perpetuity. It is made available under aCC-BY-NC-ND 4.0 International license.

to shorter wavelengths than to longer ones (*18*, *27*, *28*). Thus, the iris should be very efficient in reflecting shorter wavelength, while still being able to reflect lower levels of longer wavelengths. The two superimposed layers in the iris provide an elegant solution to these requirements. The ordered layer has a peak reflectance for shorter wavelengths and the disordered layer scatters most wavelengths, but to a lesser extent. The organization of the plate-like crystals in the ordered layer changes considerably in different regions of the iris. The crystals in the center of the iris are parallel to the iris surface, whereas at the edges they are perpendicular to the surface. This high-order organization allows the iris to efficiently block laterally impinging light and reduces spherical aberration. As mentioned, the co-orientation of the crystals allows for flawless tiling across the iris surface, thereby providing a tight seal for light. Interestingly, in certain albino fish the peripheral rods evade light damage although the inner iris epithelium lacks melanin, suggesting that the iris *argenta* also provides sufficient light screening to protect these photoreceptors (*29*).

Our analyses of the developing iris may explain the evolutionary choice of a reflective rather than absorptive iris in fish. The diameter of the 5 dpf larval eye is approximately 150 µm, increasing up to ~350 µm at 21 dpf. Taking into account the volume of the other eye parts, the space that the iris may occupy is very limited. An ordered reflecting layer is compact and, thus, advantageous under these conditions. Indeed, we found that the ordered reflecting layer, which is only ~3 µm thick, provides about 60% reflection of the blue-green light. In comparison, a melanin-based iris would require a layer of about 15 µm in thickness to absorb a similar amount of light (*30*).

Lastly, the ordered crystal layer, which mostly reflects blue-green light, is advantageous because these wavelengths are the most abundant in the marine environment. The increase in iris reflectivity with age is mostly due to increase in the coverage area by iridophores, but probably also due to the thickening of the ordered reflecting layer. The thin layer of ordered reflectors blocks a sufficiently broad spectrum of light and should allow the developing larvae to form an image, albeit of low contrast, at a very early age. The second disordered layer, which develops later, scatters a broader spectrum of light and, thereby, enables the formation of clearer images of higher contrast. This developmental strategy enables the eye to become functional at a very early stage and remain functional throughout development, as iris efficiency increases.

bioRxiv preprint doi: https://doi.org/10.1101/240028; this version posted December 28, 2017. The copyright holder for this preprint (which was not certified by peer review) is the author/funder, who has granted bioRxiv a license to display the preprint in perpetuity. It is made available under aCC-BY-NC-ND 4.0 International license.

The fish iris is an exquisite example of nature's remarkable engineering, where the specialized iridophores produce an efficient light reflector made of guanine-based crystals. We provide a biophysical mechanism for the dual functionality of the iris, an efficient light barrier and a camouflage for the fish eye. The complex optical response of the iris is achieved by a combination of wavelength-dependent light reflection from the ordered layer, scattering by the disordered layer, and absorption by the pigmented layer. The high-order organization of the reflecting layer both optimizes the light reflection properties of the iris, stops laterally impinging light, and provides the eye with camouflage. From an evolutionary-developmental perspective, the drive for developing a reflective iris could have been the small size of the eye during early development, which favors the more compact reflecting iris over the absorbing one for preventing light from reaching the retina.

References:

1. G. S. Brindley, *Physiology of the retina and the visual pathway*. Physiology of the retina and the visual pathway. (Williams and Wilkins, Oxford, England, 1960).
2. G. L. Walls, *The vertebrate eye and its adaptive radiation*. The vertebrate eye and its adaptive radiation. (Cranbrook Institute of Science, Oxford, England, 1942), pp. xiv, 785-xiv, 785.
3. I. A. Menon, S. Persad, H. F. Haberman, C. J. Kurian, P. K. Basu, A qualitative study of the melanins from blue and brown human eyes. *Exp. Eye. Res.* **34**, 531-537 (1982).
4. J. N. Lythgoe, J. Shand, Changes in spectral reflexions from the iridophores of the neon tetra. *J. Physiol.* **325**, 23-24 (1982).
5. H. B. Collin, S. P. Collin, Ultrastructure and organisation of the cornea, lens and iris in the pipefish, Corythoichthyes paxtoni (Syngnathidae, Teleostei). *Histol. Histopathol.* **10**, 313-323 (1995).
6. Y. Somiya, Fishes with eye shine: functional morphology of guanine type tapetum lucidum. *Mar. Ecol. Prog. Ser.* **2**, 9-26 (1980).
7. K. A. Soules, B. A. Link, Morphogenesis of the anterior segment in the zebrafish eye. *BMC. Dev. Biol.* **5**, 12 (2005).
8. M. P. Gray, R. S. Smith, K. A. Soules, S. W. John, B. A. Link, The aqueous humor outflow pathway of zebrafish. *Invest. Ophthalmol. Vis. Sci.* **50**, 1515-1521 (2009).
9. E. J. Denton, J. A. C. Nicol, A Survey of Reflectivity in Silvery Teleosts. *J. Mar. Biol. Assoc.***46**, 685-691 (1966).
10. E. J. Denton, M. F. Land, Mechanism of reflexion in silvery layers of fish and cephalopods. *Proc. R. Soc. London, Ser. B* **178**, 43-61 (1971).
11. E. J. Denton, Review lecture: on the organization of reflecting surfaces in some marine animals. *Philos. Trans. R. Soc. London, Ser. B* **258**, 285-313 (1970).
12. D. Gur *et al.*, The mechanism of color change in the Neon Tetra fish: a light-induced tunable photonic crystal array. *Angew. Chem. Int. Edit.* **54**, 12426-12430 (2015).
13. D. Gur *et al.*, Guanine-based photonic crystals in fish scales form from an amorphous precursor. *Angew. Chem. Int. Ed.* **52**, 388-391 (2013).
14. D. Gur, B. Leshem, D. Oron, S. Weiner, L. Addadi, The structural basis for enhanced silver reflectance in Koi fish scale and skin. *J. Amer. Chem. Soc.* **136**, 17236-17242 (2014).
15. M. Hirata, K. Nakamura, S. Kondo, Pigment cell distributions in different tissues of the zebrafish, with special reference to the striped pigment pattern. *Dev. Dyn.* **234**, 293-300 (2005).
16. S. S. Easter, Jr., G. N. Nicola, The development of vision in the zebrafish (Danio rerio). *Dev. Biol.* **180**, 646-663 (1996).
17. V. C. Fleisch, S. C. F. Neuhauss, Visual Behavior in Zebrafish. *Fish. Physiol.* **3**, 191-201 (2006).

bioRxiv preprint doi: https://doi.org/10.1101/240028; this version posted December 28, 2017. The copyright holder for this preprint (which was not certified by peer review) is the author/funder, who has granted bioRxiv a license to display the preprint in perpetuity. It is made available under aCC-BY-NC-ND 4.0 International license.

18. S. C. F. Neuhauss, Zebrafish Vision: Structure and Function of the Zebrafish Visual System. *Fish. Physiol.* **29**, 81-122 (2010).
19. M. Bernhardt *et al.*, Anisotropic x-ray scattering and orientation fields in cardiac tissue cells. *New J. Phys.* **19**, 013012 (2017).
20. J. D. Nicolas *et al.*, Scanning X-ray diffraction on cardiac tissue: automatized data analysis and processing. *J. Synchrotron Radiat.* **24**, 1163-1172 (2017).
21. M. Inaba, H. Yamanaka, S. Kondo, Pigment pattern formation by contact-dependent depolarization. *Science* **335**, 677 (2012).
22. D. S. Eom, E. J. Bain, L. B. Patterson, M. E. Grout, D. M. Parichy, Long-distance communication by specialized cellular projections during pigment pattern development and evolution. *Elife* **4**, (2015).
23. H. Hamada *et al.*, Involvement of Delta/Notch signaling in zebrafish adult pigment stripe patterning. *Development* **141**, 318-324 (2014).
24. U. Irion *et al.*, Gap junctions composed of connexins 41.8 and 39.4 are essential for colour pattern formation in zebrafish. *Elife* **3**, e05125 (2014).
25. S. Johnsen, *The optics of life: a biologist's guide to light in nature*. (Princeton University Press, 2012).
26. C. Lalli, T. R. Parsons, *Biological oceanography: an introduction*. (Butterworth-Heinemann, 1997).
27. W. T. Allison, T. J. Haimberger, C. W. Hawryshyn, S. E. Temple, Visual pigment composition in zebrafish: Evidence for a rhodopsin-porphyropsin interchange system. *Vis. Neurosci.* **21**, 945-952 (2004).
28. D. A. Cameron, Mapping absorbance spectra, cone fractions, and neuronal mechanisms to photopic spectral sensitivity in the zebrafish. *Vis. Neurosci.* **19**, 365-372 (2002).
29. D. M. Allen, Peripheral rods evade light damage in albino trout. *Invest. Ophth. Vis. Sci.* **38**, 4787-4787 (1997).
30. E. V. Koblova, A. N. Bashkatov, E. A. Genina, V. V. Tuchin, V. V. Bakutkin, Estimation of melanin content in iris of human eye. *.P Soc. Photo-Opt. Ins.* **5688**, 302-311 (2005).
31. D. Gur *et al.*, Structural basis for the brilliant colors of the Sapphirinid copepods. *J. Amer. Chem. Soc.* **137**, 8408-8411 (2015).
32. A. Hirsch *et al.*, *Chem. Mat.* **27**, 8289-8297 (2015).

Acknowledgments: We Thank Dr. Nadav Elad for his help with the TEM Studies and Dr. Eyal Shimoni and Dr. Ifat Kaplan-Ashiri for their help with the SEM Studies. We thank Tal Bigdary for graphical schemes. We acknowledge the European Synchrotron Radiation Facility for provision of synchrotron radiation facilities and we would like to thank Manfred Burghammer for assistance in using beamline ID13 – microfocus beamline. We are also very thankful for helpful advice on the x-ray data analysis by Prof. Dr. Tim Salditt, Institute for X-ray Physics, Göttingen, Germany. This work was supported the Crown Center of Photonics, and the I-CORE (Israeli Center for Research Excellence) "Circle of Light", the Israel Science Foundation (#1511/16); F.I.R.S.T. (Bikura) Individual Grant (#2137/16); Israel Ministry of Agriculture Chief Scientist Office (#894-0194-13 and #30-04-0002); minerva-Weizmann program and Adelis Metabolic Research Fund, (in the frame of the Weizmann Institute). G.L. is an incumbent of the Elias Sourasky Professorial Chair.